Iron Loss Reduction Method of V/f Control for Switched Reluctance Motor

Hirotaka Kato[1], Hiroki Watanabe[1], and Jun-ichi Itoh[1]

[1] Nagaoka University of Technology, Japan

***Abstract*-- This paper proposes an iron loss reduction method in a V/f control for a switched reluctance motor (SRM). The proposed method applies the three-level modulation method to reduce harmonic iron loss. In addition, a reactive power compensation control of the proposed strategy eliminates fundamental iron loss caused by a reactive power. The proposed method reduces 69.0% of the harmonic iron loss and 4.7% of the fundamental iron loss in the experiment.**

***Keywords*— Iron loss, Switched reluctance motor, V/f control**

I. Introduction

A switched reluctance motor (SRM) is composed of only an iron core and windings without a permanent magnet using a rare earth, which is inexpensive to manufacture. The SRM has attracted attention as a variable-speed motor for industrial applications due to the robust salient pole structure of its rotor [1][2]. The variable-speed drive without a position sensor is expected for the SRM to take advantage of the high-temperature and high-speed durability and cost-effectiveness.

Many studies have been conducted on the rotor position sensorless drive methods with the estimated position using the position dependency of inductance [3-6]. In these methods, the instantaneous value of the inductance is first calculated from the voltage and current. Then, the calculated inductance is converted into the rotor position information with a look-up table or an approximation formula of the relationship between inductance and rotor position. However, these methods require complicated controls such as harmonic voltage superposition [3][4] or additional analog circuits [5][6] to detect the instantaneous inductance accurately. The authors have proposed a V/f control for the SRM in order to overcome the above disadvantages [7]. The V/f control does not require the rotor position information because it is based on the rotating coordinate system with respect to the inverter output voltage. Therefore, the V/f control does not have the accuracy problems of the inductance detection and the rotor position conversion essentially.

The reduction of both the copper loss and iron losses is important to achieve the high-efficiency drive of the SRM. The maximum torque/ampere control is proposed assuming that the controller for the SRM is based on a mathematical model, such as field-oriented control (FOC) and the V/f control [8]. Although this method minimizes the copper loss by minimizing the RMS current, the iron loss increases with the speed of the motor. The iron loss in high-speed operation can be a significant problem in the SRM since it is expected to be applied for high-speed rotation applications [9-11]. The iron loss is divided into the harmonic iron loss caused by the switching operation of the inverter and the fundamental iron loss caused by fundamental voltage [11]. Different approaches are required to reduce both fundamental iron loss and harmonic iron loss.

Ref. [12] has reduced the iron loss by optimizing the conduction timing for the hysteresis current control. However, this method requires a trial-and-error approach to optimize the control parameters, which make the implementation complicated. Therefore, it is not easy to implement the SRM control based on the mathematical model. In addition, the iron loss reduction method is proposed for the FOC of the synchronous reluctance motor, which adjusts the excitation current depending on the torque [13]. However, this method also cannot be applied with the V/f control because the V/f control does not have a torque controller.

This paper proposes an iron loss reduction method in the V/f control for the SRM. The fundamental iron loss and the harmonic iron loss are reduced by the proposed method. The proposed method consists of two approaches, (i)applying the three-level modulation method: the harmonic ripple in the flux density is reduced by applying the three-level modulation to the asymmetrical half-bridge converter, (ii)reactive power compensation control: the fundamental amplitude of the flux density is reduced by compensating the reactive power command based on the maximum torque/ampere control. This paper describes first (i) and then (ii).

II. Iron Loss Reduction Method of V/f Control for SRM

Fig.1 shows the control diagram of the V/f control for the SRM. The V/f control consists of (A)zero-phase current control, (B)V/f control and damping control, and

(C)high-efficiency control [7]. This paper reduces the iron loss by adding the following two parts to the V/f control, (i)the three-level modulation method and (ii)reactive power compensation control.

A. Reduction Method of Harmonic iron loss

Fig.2 shows the operating principles of the two-level and three-level modulation methods. Fig.3 shows the waveform of each modulation method. The two-level modulation method, as shown in Fig.2(b), is generally adopted to drive the SRM with the voltage command [8][14]. The iron loss is formulated with the Improved Generalized Steinmetz Equation (iGSE) [15] as

$$\begin{cases} P_{\mathrm{V}} = \dfrac{1}{T}\displaystyle\int_0^T k_i \left|\dfrac{dB(t)}{dt}\right|^{\alpha} (\Delta B)^{\beta-\alpha}\, dt \\ k_i = \dfrac{k}{(2\pi)^{\alpha-1}\displaystyle\int_0^{2\pi} \left|\cos\theta\right|^{\alpha} 2^{\beta-\alpha}\, d\theta} \end{cases} \tag{1}$$

where

$$\frac{dB(t)}{dt} = \begin{cases} \dfrac{E_{dc}}{NA} & V(t) = E_{dc} \\ 0 & V(t) = 0 \\ -\dfrac{E_{dc}}{NA} & V(t) = -E_{dc} \end{cases} \tag{2}$$

where P_{v} is the iron loss per unit volume, T is the one period of the electric angle, k, α, β is the Steinmetz coefficient, B is the flux density of the stator core, ΔB is the peak-to-peak of B, $V(t)$ is the output voltage of the inverter, E_{dc} is the DC voltage of the inverter, N is the number of turns of the slot winding, and A is the effective cross-section. According to (1), the iron loss is generated when the inverter output voltage $V(t)$ is $\pm E_{\mathrm{dc}}$ and becomes zero when $V(t)$ is zero [16]. The flux density oscillates, as shown in Fig.3(a) because the applied voltage is only E_{dc} or $-E_{\mathrm{dc}}$ when the two-level modulation method is used. On the other hand, the three-level modulation method shown in Fig.2(c) outputs not only $\pm E_{\mathrm{dc}}$ but also zero by fixing the switching state of either the upper or lower arm to ON or OFF during the half of the electric period. The iron loss is not generated during the zero-voltage period because dB/dt shown in (2) becomes zero. In particular, the iron loss of the three-level modulation is reduced significantly in operation with a low modulation index because the zero-voltage period becomes longer as the modulation index decreases.

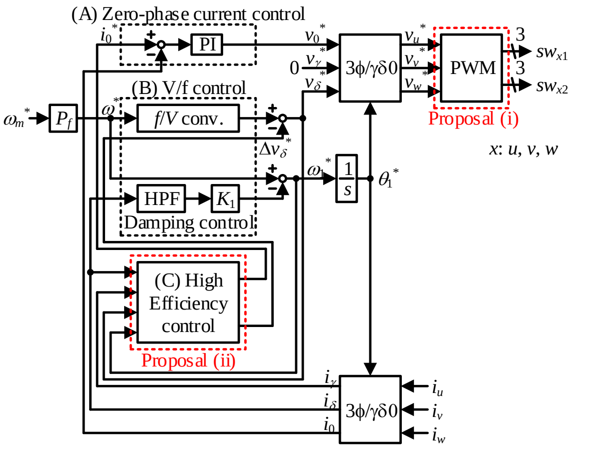

Fig. 1. V/f control method based on γδ axis.

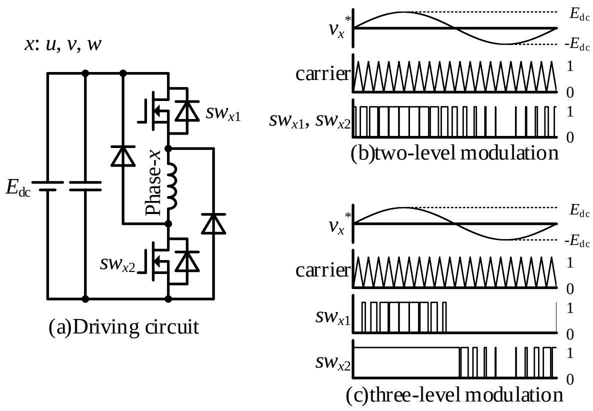

Fig. 2. Operating principals
Between two-level and three-level modulation.

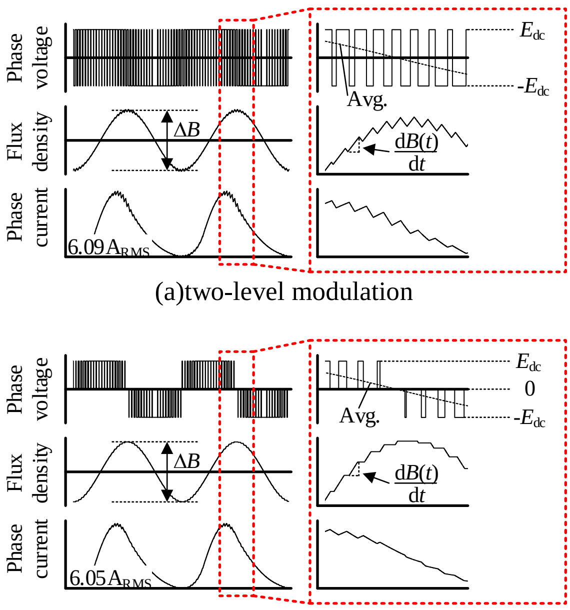

Fig. 3. Comparison of waveform
between two-level and three-level modulation.

B. Reduction Method of Fundamental iron loss

Fig.4 shows the control diagram of the reactive power compensation control. This control module is based on the maximum torque/ampere control using reactive power feedback. The maximum torque/ampere control is explained first, followed by the reactive power compensation control. The condition of the maximum torque/ampere ratio of the SRM is expressed by the following equation [8].

$$\begin{cases} i_0 = \sqrt{2} i_q \\ i_d = 0 \end{cases} \tag{3}$$

where i_d, i_q, i_0 is the dq0-axis current, $\sqrt{2}$ means the coefficient in the park transformation. Note that the zero-phase current is larger than the AC current amplitude because the negative current does not flow due to the asymmetrical half-bridge converter. Therefore, it is necessary to satisfy not only i_d=0 but also i_0=i_q for the condition of the maximum torque/ampere ratio.

First, the i_0=i_q control is explained. i_q is equal to the amplitude of the AC current I_{ac} when i_d=0. Thus, i_0 is controlled to $\sqrt{2}\,I_{ac}$ so that the negative current does not flow. The command value of the zero-phase current control is expressed as (4).

$$i_0^{\ *} = \sqrt{2} i_q = \sqrt{2} I_{ac} = \sqrt{2} \sqrt{i_\gamma^{\ 2} + i_\delta^{\ 2}} \tag{4}$$

where i_γ and i_δ are the γ and δ-axis currents, respectively. As shown in Fig.4, the value calculated by (4) is used as the reference value for zero-phase current control for the i_0=i_q control.

Next, the i_d=0 control is explained. The i_d=0 control is achieved indirectly in the γδ coordinate by the feedback of the reactive power of the SRM. In the dq-axis coordinate, the reactive power Q_{dq} injected into the SRM is expressed as in (5).

$$Q_{dq} = v_q i_d - v_d i_q = 2\omega \left\{ L_{dc} (i_d^{\ 2} + i_q^{\ 2}) + L_{ac} i_0 i_d \big/ \sqrt{2} \right\} \tag{5}$$

where v_d and v_q are the d-axis and q-axis currents, respectively. The reactive power Q_{dq} under the condition of i_d=0 is expressed in (6).

$$Q_{dq} = 2\omega L_{dc} i_q^{\ 2} = 2\omega L_{dc} I_{ac}^{\ 2} = 2\omega L_{dc} (i_\gamma^{\ 2} + i_\delta^{\ 2}) \tag{6}$$

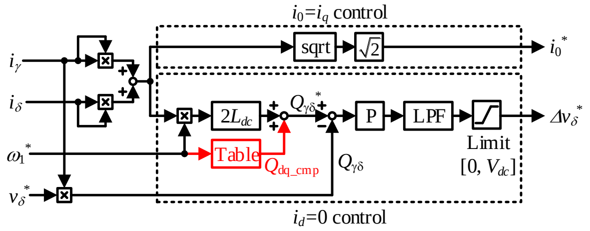

Fig. 4. Control diagram of high-efficiency control.

On the other hand, in the coordinate γδ-axis, the reactive power $Q_{\gamma\delta}$ is expressed as in (7).

$$Q_{\gamma\delta} = v_\delta i_\gamma \tag{7}$$

On the other hand, the deviation between (6) and (7) is regulated to zero by adjusting the v_δ with the P controller for i_d=0 control. Note that the low pass filter (LPF) in the second stage of the P controller shown in Fig.2 reduces the loop gain at high frequency to achieve i_d=0 only the steady state [17-20]. In addition, a limit is provided to prevent overcompensation.

Finally, the reactive power compensation control is explained. Although the maximum torque/ampere control can minimize the copper loss, the iron loss is not considered. This paper minimizes the sum of the copper loss and the iron loss. According to (1), the iron loss increases depending on ΔB. ΔB decreases as v_δ decreases, which can be achieved by reducing the modulation index in the V/f control. In the reactive power compensation control, the reactive power command $Q_{\gamma\delta}$ is modified by the additional term Q_{dqref_cmp} as

$$Q_{\gamma\delta}^* = Q_{dqref\_cmp} + 2\omega L_{dc} \left(i_\gamma^2 + i_\delta^2 \right) \tag{8}$$

Negative Q_{dqref_com} reduces v_δ and results in the reduction of iron loss [21].

Table 1 shows the parameter of the SRM in the experiment. Fig.5 shows the experimentally measured loss with respect to Q_{dqref_cmp}. Fig.6 shows Q_{dqref_cmp} that minimizes the total loss at different speeds from the experimental results. The loss breakdown method in Fig.5 is explained below. In this paper, the total loss is defined as a sum of the mechanical loss, the copper loss, and the iron loss. The mechanical loss is estimated from the output torque when the test motor is driven by the load motor. The copper loss is calculated from the winding resistance considering the temperature dependency and the RMS current measured by a power meter. The iron loss is determined by subtracting the mechanical power, mechanical loss, and copper loss from the motor input power. As mentioned above, Q_{dqref_cmp} is set to a negative value to make v_δ lower than that in the maximum torque/ampere control. Compared to the condition of maximum torque/ampere ratio, negative Q_{dqref_cmp} reduces the iron loss while increasing the copper loss. Since the iron loss is frequency dependent, Q_{dqref_cmp} that minimizes the total loss is speed dependent. The optimum Q_{dqref_cmp} is referred from the table so that Q_{dqref_cmp} is adjusted according to the speed when implementing the V/f control.

Table 1. Motor parameters

Rated power	2.2kW
Base speed(1p.u.), Max. speed	4800rpm, 7200rpm
Max. torque(1p.u.)	4.38Nm
DC voltage	300V
Poles	Stator:18, Rotor:12
Inertia	62.3×10^{-4}kgm^2
Resistance	0.45Ω
DC inductance	7.82mH
AC inductance	5.19mH
Rated current(1p.u.)	7.7A(i_{0Max}, i_{qMax})

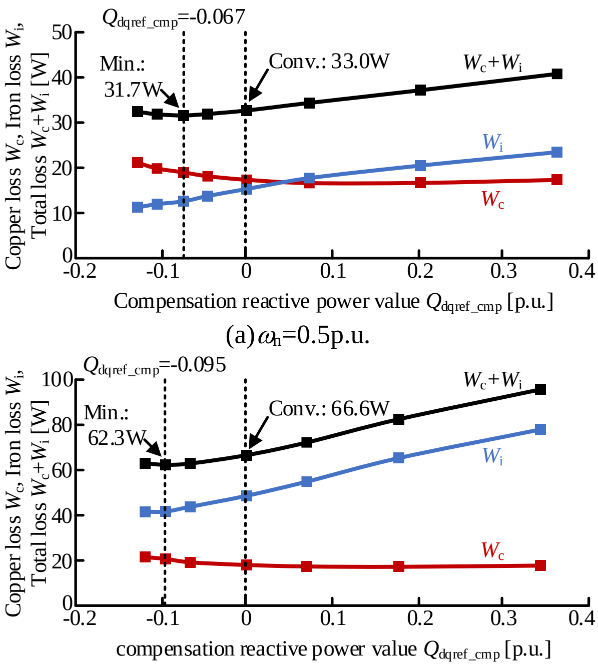

(a) ω_h=0.5p.u.

(b) ω_h=1.5p.u.

Fig. 5. Relationship between Q_{dq_cmp} and the total loss (Torque=0.1p.u.)

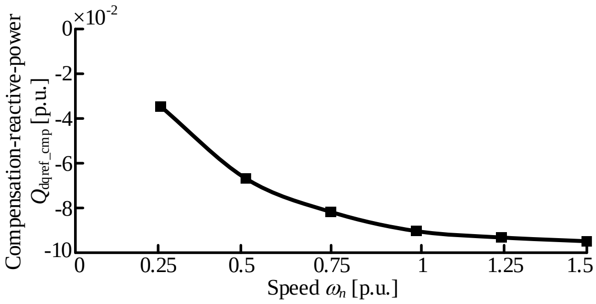

Fig. 6. Relationship between ω_n and Q_{dqref_cmp} when the total loss minimum (Torque=0.1p.u.)

III. Experimental Results

Fig. 7 and Fig.8 show the comparison of the current and the loss with the two-level modulation and the three-level modulation. The harmonic ripple caused by the switching is suppressed by the three-level modulation in Fig.7(b) compared with the two-level modulation in Fig.7(a). As a result, the application of the three-level modulation reduces the iron loss by 52.8%, whereas the reduction of the copper loss is relatively small as shown in Fig.8. In other words, a reduction of the harmonic iron loss is achieved.

Fig.9 shows the loss comparison results when (A): the two-level modulation and the maximum torque/ampere control, (B): the three-level modulation and the maximum torque/ampere control, and (C): the three-level modulation and the reactive power compensation control, are applied. Fig. 10 compares the breakdown results of the measured loss at 0.25p.u. and 1.5p.u. speed among (A), (B), and (C). Fig.11 shows the current waveform when (B) or (C) is applied. According to Fig.9 and Fig.10, the loss is reduced by up to 69.0% by changing the modulation method and by up to 4.7% by applying the reactive power compensation control. The effect of the iron loss reduction at 0.25p.u. speed is better than that at 1.5p.u. speed, as shown in the comparison between (A) and (B). This is because the modulation index at 0.25p.u. speed is lower than that at 1.5p.u. speed, which generates longer periods of zero-voltage, as aforementioned in section II.A. On the other hand, the effect of the iron loss reduction at 1.5p.u. speed is better than that at 0.25p.u. speed, as shown in the comparison between (B) and (C). This is because the ratio of the fundamental iron loss in the total loss increased as the fundamental frequency increased. In addition, a comparison of Fig.11(a) and (b) reveals that the RMS currents are almost the same, which is due to the small

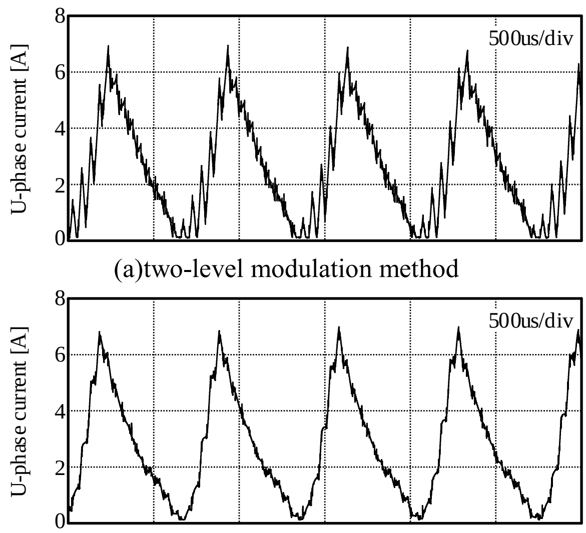

(a)two-level modulation method

(b)three-level modulation method

Fig.7. Current waveform with each modulation method when each modulation method is applied.

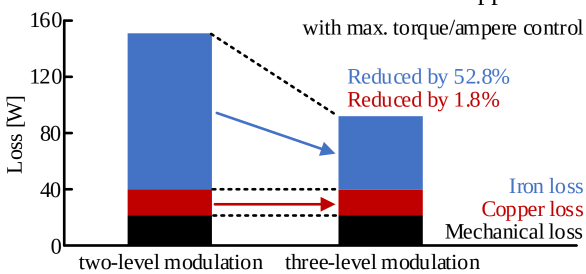

Fig. 8. Loss comparison between two-level and three-level modulation (ω_n=1.5p.u., Torque=0.1p.u.).

Q_{dqref_cmp} shown in Fig.6. On the other hand, the RMS current in Fig.11(d) is higher than that in Fig.11(c) because the Q_{dqref_cmp} is set to the small value in order to minimize the total losses. It is concluded that the proposed method reduces both the harmonic iron loss and the fundamental iron loss, which are clarified by the comparison between (A) and (B) and by the comparison between (B) and (C), respectively.

IV. Conclusions

This paper proposed the iron loss reduction method of the V/f control for the SRM. The harmonic iron loss is reduced by changing the modulation method from the two-level modulation to the three-level modulation. In addition, the fundamental iron loss is reduced by applying the reactive power compensation control. From the experimental results, it was confirmed that the harmonic iron loss is reduced by 69.0% at maximum with the three-level modulation, and the fundamental iron loss is reduced by 4.7% with the reactive power compensation control.

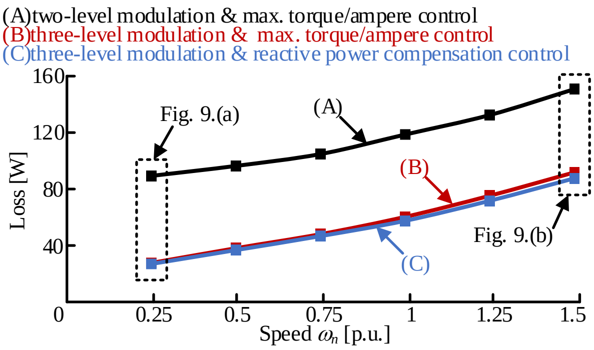

Fig. 9. Loss comparison between 3 methods (Torque=0.1p.u.).

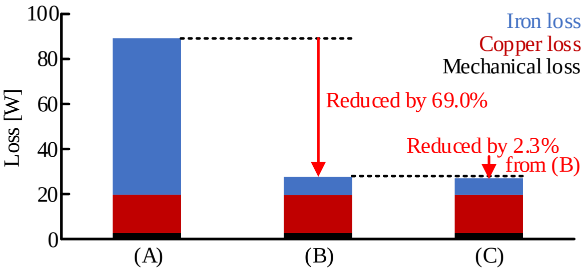

(a) ω_n=0.25p.u.

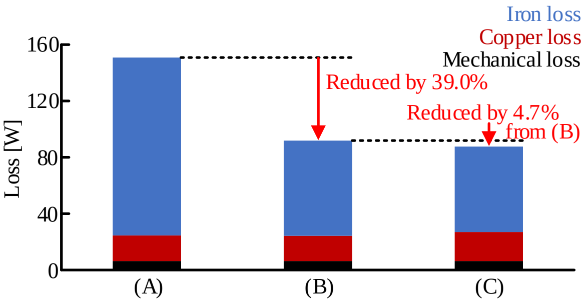

(b) ω_n=1.5p.u.

Fig. 10. Comparison by Loss separation (Torque=0.1p.u.).

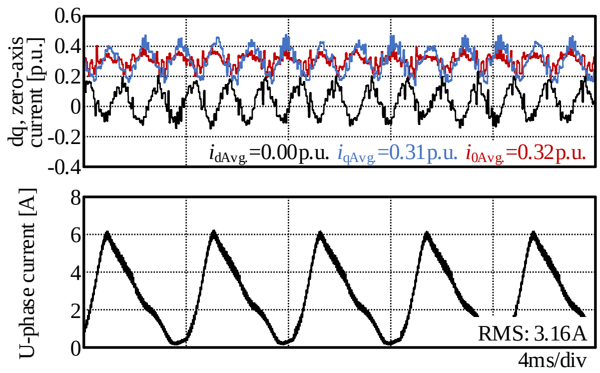

(a) When (B) is applied (ω_n=0.25p.)

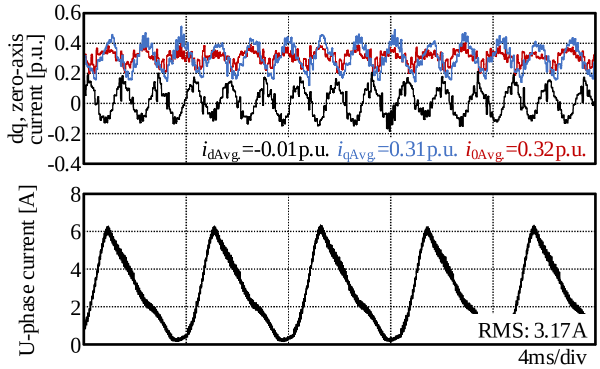

(b) When (C) is applied (ω_n=0.25p.u.)

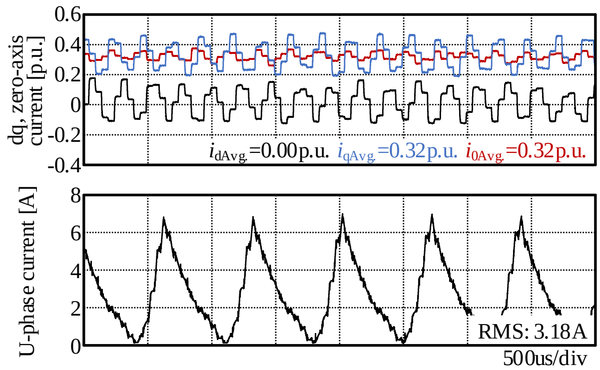

(c)When (B) is applied (ω_n=1.5p.u.)

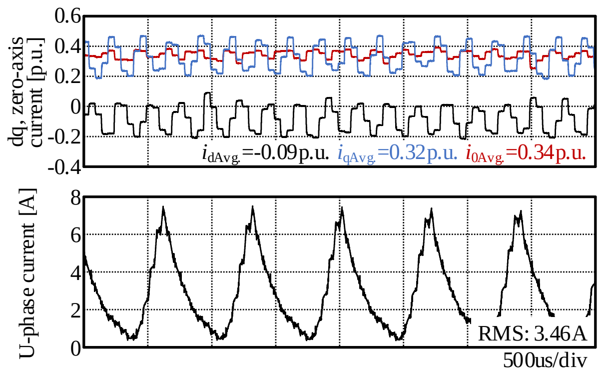

(d)When (C) is applied (ω_n=1.5p.u.)

Fig. 11. Current waveform with (B) and (C) (Torque=0.1p.u.).

References

[1] T. Kosaka, A. Kume, H. Wakayama, and N. Matsui: "Development of high torque density and efficiency switched reluctance motor with 0.1mm short airgap", in Proceedings of the IEEE European Conference on Power Electronics and Applications 2007, pp. 1–9 (2007)

[2] H. Yamai, Y. Sawada, and K. Ohyama: "Applying Switched Reluctance Moor to Oil Hydraulic Pump Use", IEEJ Journal Industry Applications, vol. 123, no. 2, pp. 96-104 (2014)

[3] K. -W. Hu, Y.-Y. Chen, and C.-M. Liaw: "A reversible position sensorless controlled switched-reluctance motor drive with adaptive and intuitive commutation tunings", IEEE Transactions on Power Electronics, Vol.30, No.7, pp.3781-3793 (2015)

[4] K. Ha, R.Y. Kim, and R. Krishnan: "Position estimation in switched reluctance motor drive using the first switching harmonics through Fourier series", IEEE Transactions on Industrial Electronics, Vol.58, No.12, pp.5352–5360 (2011)

[5] G.G. Lopez, P.C. Kjaer, and T.J.E. Miller: "A new sensorless method for switched reluctance motor drives", IEEE Transactions on Industry Applications, Vol.34, No.4, pp.832–840 (1998)

[6] S. Sumita, K. Deguchi, and Y. Iwaji: "Position Sensorless Control Method for SRM Using Analog Circuit of Type-1 Control System", IEEJ Transactions on Industry Applications, Vol.137, No. 8, pp.612-621 (2017)

[7] T. Kumagai, J. Itoh, M. Kato, "V/f Control for Switched Reluctance Motor," 2022 IEEE Energy Conversion Congress and Exposition (ECCE), Detroit, MI, USA, 2022, pp. 1-6 (2022)

[8] N. Nakao, K. Akatsu: "Vector Control Specialized for Switched Reluctance Motor Drives", IEEJ Transactions of Industry Applications, Vol.134, No.12, pp.1006-1015 (2014)

[9] V. Raulin, A. Radun, I. Husain: "Modeling of Losses in Switched Reluctance Machines", IEEE Transactions on Industry Applications, Vol. 40, No. 6, pp.1560-1569 (2004)

[10] H. Hayashi, K. Nakamura, A. Chiba, T. Fukao, K. Tungpimolrut, D. G. Dorrell: "Efficiency Improvements of Switched Reluctance Motors with High-Quality Iron Steel and Enhanced Conductor Slot Fill", IEEE Transactions on Energy Conversion, Vol.24, No.4, pp. 819-825 (2009)

[11] Q. Yu, B. Bilgin, A. Emadi, "Loss and Efficiency Analysis of Switched Reluctance Machines Using a New Calculation Method", IEEE Transactions on Industrial Electronics, Vol. 62, No. 5, pp3072-3080 (2015)

[12] Y. Nakazawa, K. Ohyama, H. Fujii, H. Uehara, Y. Hyakutake: "Efficiency Improvement of Switched Reluctance Motor by Single-Pulse Control with Variable Excitation Period", Vol. 135, No.3, pp284-290 (2014)

[13] R. Hiyoshi, T. Noguchi: "Maximum Efficiency Operation of Synchronous Reluctance Motor Using Mathematical Models of Magnetic Saturation and Iron-Core Loss Characteristics", 2013 IEEJ Annual Meeting, No. 4-114 (2013)

[14] R. Shi, H. A. Toliyat: "Vector control of five-phase synchronous reluctance motor with space vector pulse width modulation (SVPWM) for minimum switching losses", APEC. Seventeenth Annual IEEE Applied Power Electronics Conference and Exposition, Vol.1, pp. 57-63 (2002)

[15] J. Muhlethaler, J. Biela, J. W. Kolar, A. Exklebe: "Improved Core-Loss Calculation for Magnetic Components Employed in Power Electronic Systems", IEEE Transactions on Power Electronics, Vol. 27, No. 2, pp. 964-973 (2012)

[16] T. Kumagai, T. Itoh, K. Nishikawa, J. Itoh, K. Yamane, M. Nawa: "Reduction of Iron Loss in Stator Core using an Optimum Pulse Pattern for High-Speed IPMSM", IEEJ Transactions on Industry Applications, Vol. 141, No. 4, pp. 313-323 (2021)

[17] J. Itoh, N. Nomura, and H. Ohsawa, "A comparison between V/f control and position-sensorless vector control for the permanent magnet synchronous motor", Proceedings of the Power Conversion Conference-Osaka 2002, Vol.3, pp.1310-1315 (2002)

[18] J. Itoh, T. Toi, M. Kato: "Maximum Torque per Ampere Control Using Hill Climbing Method Without Motor Parameters Based on V/f Control", 18th European Conference on Power Electronics and Applications (EPE'16), No. DS3d-Topic 4-0283, (2016)

[19] J. Itoh, T. Toi, K. Nishizawa: "Stabilization Method Using Equivalent Resistance Gain Based on V/f Control for IPMSM with Long Electrical Time Constant", The 2018 International Power Electronics Conference, No. 23E1-5, pp. 2229-2236 (2018)

[20] J. Itoh, T. Toi, K. Nishizawa: "Stabilization Method for IPMSM with Long Electrical Time Constant Using Equivalent Resistance Gain Based on V/f Control", IEEJ Transactions on Industry Applications, Vol. 8, No. 4, pp. 592-599 (2019)

[21] J. Itoh, Y.Nakajima, G.T.Chiang: "Maximum Torque per Ampere and Maximum Efficiency Control Methods based on V/f Control for IPM Synchronous Motors", IEEJ Journal of Industry Applications, Vol. 3, No. 2, pp. 112-120 (2013)